THE RELATIONSHIP BETWEEN IR, OPTICAL, AND UV EXTINCTION

Jason A. Cardelli, Geoffrey C. Clayton, and John S. Mathis
Department of Astronomy, University of Wisconsin
Madison, Wisconsin 53706 USA

ABSTRACT: We present an analysis of the variability of absolute IR, optical, and UV extinction, A_λ, derived through the ratio of total-to-selective extinction, R [$\equiv A_V/E(B-V)$], for 31 lines of sight for which reliable UV extinction parameters have been derived. These data sample a wide range of environments and are characterized by $2.5 \leq R \leq 6.0$. We find that there is a strong linear dependence between extinction expressed as A_λ/A_V and R^{-1} for $1.25\ \mu m \leq \lambda \leq 0.12\ \mu m$. Differences in the general shape of extinction curves are largely due to variations in shape of optical/near-UV extinction ($\lambda \leq 0.7\ \mu m$) corresponding to changes in R, with A_λ/A_V decreasing for increasing R. From a least-squares fit of the observed R-dependence as a function of wavelength for $0.8\ \mu m^{-1} \leq \lambda^{-1} \leq 8.3\ \mu m^{-1}$, we have generated an analytic expression from which IR, optical, and UV extinction curves of the form A_λ/A_V can be reproduced with reasonable accuracy from a knowledge of R. We also find that the absolute bump strength normalized to A_V shows a general decrease with increasing R, suggesting that some fraction of bump grains may be selectively incorporated into coagulated grains. Finally, we find that *absolute extinction* normalized by suitably chosen color indices [e.g. $E(\lambda_1-\lambda_2)$] results in a minimization of the R-dependence of portions of the UV curve, allowing A_λ to be estimated for these wavelengths independent of R.

1. INTRODUCTION

Interpretation of the variability of observed extinction, particularly in the UV, has been confused because most extinction data must be compared in a *relative* way [e.g. $E(\lambda-V)/E(B-V)$], and thus the true nature of the variability may be obscured by the normalization. Conversion of normalized extinction curves to absolute data requires knowledge of the ratio of total-to-selective extinction, R [$\equiv A_V/E(B-V)$]. Clayton and Mathis (1988) have shown that, longward of 0.7 μm, the shape of extinction curves are generally the same and are independent of R. Changes in R arise in the optical/near-UV portion of the curve as a flattening of the observed extinction.

In this paper we examine the variations between R and various UV extinction parameters derived by Fitzpatrick and Massa (1986, 1988; FM88). This represents a continuation of work presented by Cardelli, Clayton, and Mathis (1988a,b). We utilize the data of 31 stars from FM88 for which optical and IR data also exist. For the UV data, FM88 fitted observed extinction curves of the form $E(\lambda-V)/E(B-V)$ with three components; a linear ($1/\lambda$) background, a Lorentzian-like 2175 Å bump in the form of an assumed "Drude function", and a far-UV cubic polynomial. While some aspects of such a parameterization may be more mathematical than physical, the process does provide two

benefits. First, a parameterized curve is easy to reproduce. Second, parameterization of individual curves allows quantitative comparison of specific aspects of UV extinction such as, for example, the position and width of the bump.

The R values used here were derived by fitting the observed near-infrared/optical extinction for $\lambda > 0.7$ μm with the average curve (R = 3.08) of Rieke and Lebofsky (1985). The nature of this fit can be seen in Figure 1 of Cardelli, Clayton, and Mathis (1988a; CCM). Below we descibe the nature of the dependencies between observed extinction and R.

2. VARIABILITY OF GENERAL/TOTAL-TO-SELECTIVE EXTINCTION

2.1 A_λ/A_V versus R^{-1}: The Analytic Dependence

CCM found that there exists a strong relationship between A_λ/A_V and R^{-1} for all UV wavelengths, although the scatter is largest for $\lambda < 0.15$ μm. We have now extended that work to include the optical/near-infrared down to 1.25 μm. An example of this relationship at three wavelengths is shown in Figure 1. We must note that deviations in the shape of optical curves can extend down to and slightly longward of the V bandpass. This is readily apparent by the non-zero slope for the bottom plot in Figure 1. As a result, A_V is perhaps not the best choice, since A_λ/A_V will exhibit some R-dependence at all wavelengths. However, we use this normalization because $A_V/E(B-V)$ has historical significance and a number of the stars lack data at the *R* bandpass ($\lambda = 0.7$ μm). Besides, the deviations below V are generally small, even for lines of sight with R > 4.5.

CCM presented an analytic expression, derived from a least-squares fit between A_λ/A_V and R^{-1} as a function of x ($\equiv 1/\lambda\ \mu m^{-1}$), which can be used to generate UV extinction curves via R which are in relatively good agreement with the observed data. We have combined this with similar fits to optical data so that a complete curve can be generated for 1.25 μm $\leq \lambda \leq$ 0.12 μm. The equation has the form;

$$< A_\lambda/A_V > = a(x) + b(x)/R \qquad (1)$$

where for $0.8\ \mu m^{-1} \leq x < 3.2\ \mu m^{-1}$ *and* $y=(x-1.82)$*;*

$$a(x) = 1 + 0.15020y - 0.34376y^2 + 0.05201y^3 + 0.030339y^4 - 0.01009y^5$$

$$b(x) = 1.75496y + 0.80985y^2 - 0.26666y^3 + 0.01273y^4 - 0.00610y^5$$

and for $x \geq 3.2\ \mu m^{-1}$*;*

$$a(x) = 1.802 - 0.316x - 0.104/[(x-4.67)^2+0.341] + F_a(x)$$

$$b(x) = -3.090 + 1.825x + 1.206/[(x-4.62)^2 + 0.263] + F_b(x)$$

$$F_a(x) = -0.04473(x-5.9)^2 - 0.009779(x-5.9)^3 \qquad (x \geq 5.9)$$

$$F_b(x) = 0.2130(x-5.9)^2 + 0.1207(x-5.9)^3 \qquad (x \geq 5.9)$$

$$F_a(x) = F_b(x) = 0 \text{ for } x < 5.9 \qquad (x < 5.9)$$

Figure 2 shows a comparison between the formula and real data for three different values of R. The strong dependency of the general level of the UV extinction with R is quite apparent. HD 154445 has been shown because it represents one of the poorest fits in the sample. For the majority of cases, however, the fit is much better. For $R \approx 3.2$, we find excellent agreement between our analytic formula and the standard *average* curves in both the optical and the UV (e.g. Schild 1977; Savage and Mathis 1979; Seaton 1979; Rieke and Lebofsky 1985). However, because these curves correspond to a unique value of R, the dependency shown in Figure 2 clearly indicates that use of these curves to deredden spectra appropriate to R values different from $3.1 \leq R \leq 3.5$ would be inappropriate. Despite the apparent poor fit for HD 154445, our analytic expression for $R = 3.61$ actually reproduces the observed curve better than using an *average curve* with the same R value. Although R may not be an easy parameter to derive for a particular line of sight, these results indicate that use of the *average curve* with $R > 3.5$ can lead to large systematic errors. Similarly, it is inaccurate to use a *θ Ori-like curve* ($R \approx 5.3$) with $R < 5$.

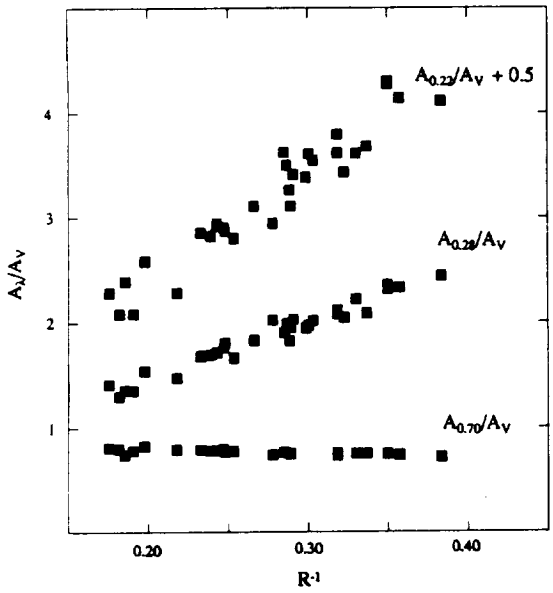

Figure 1: Absolute extinction, A_λ, normalized to A_V versus R^{-1} at three different wavelengths derived from our sample of 31 stars. The top plot has been shifted up by 0.5 units in order to separate it from the middle plot.

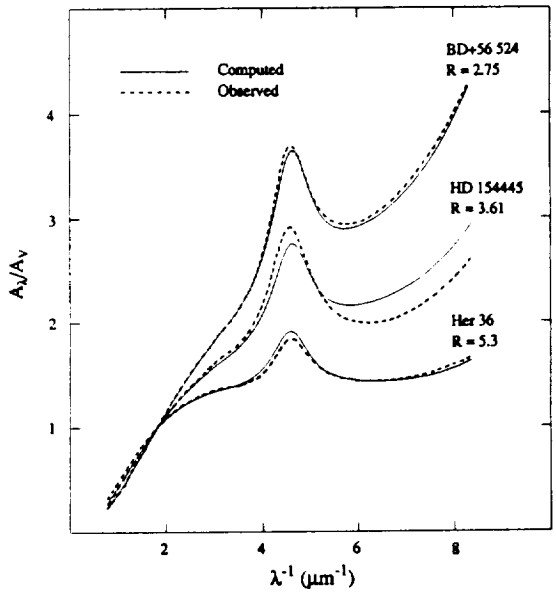

Figure 2: Comparison of the R-dependent relation (eqn. 1) derived from extinction data for the stars in our sample with observed extinction for three stars with different R values. HD 154445 represents one of the most discrepant cases.

2.2 The Variation of A_{bump}/A_V with R^{-1}: Interpretation

Figure 3 shows a comparison between R^{-1} and several UV bump parameters as derived by FM88. In Figure 3a, we find that A_{BUMP}/A_V, the *absolute bump strength* (above the linear background) *normalized by the total visual extinction*, shows a strong dependency on R^{-1} varying between 0.5 ± 0.2 at $R = 5$ and 1.25 ± 0.3 at $R = 3$ (the uncertainties represent the maximum range of the data). This general dependency on R^{-1}

does not necessarily mean that the bump arises from the same species of grains that give rise to the optical extinction. Figures 3b and 3c show plots of bump width ($\gamma \equiv$ FWHM) and central position ($1/\lambda_o$) versus R^{-1} which do not show any clear R-dependence. This would seem to indicate that the bump grains are indeed a separate component which show independent variability. However, the direct relationship between A_{BUMP}/A_V and R^{-1} could be understood qualitatively in a rather simple way. A small value of R^{-1} is most easily explained by an increase in the mean size of the grains which provide the optical extinction. This growth probably involves coagulation, in which small grains are incorporated into larger ones. In most grain models, the carrier of the bump is seen as small grains (usually graphitic carbon). It is easy to imagine that some of these grains would be incorporated into the larger ones under coagulation conditions. In such a scenario, incorporation of some fraction of the bump grains into larger grains, where they do not produce a bump, would result in a decrease in the relative bump strength through a decrease in the column density. The remaining uncoagulated grains are presumably 'free' to respond independently to environmental conditions. Mathis and Whiffen (1989) have made the above arguments quantitative, and other grain models probably could as well.

A similar relationship also exists for the far-UV component (see Cardelli, Clayton, and Mathis 1988b). FM88 found that the shape of the far-UV curvature was essentially the same for all of the stars in their sample and so derived the far-UV component by fitting a single polynomial expression with a variable scale factor. We find that this scale factor, normalized by A_V, also appears to vary with R^{-1}, although the dependence is not as well defined and there are a few lines of sight (e.g. HD 147889, HD 204827) which exhibit strong deviations from the mean.

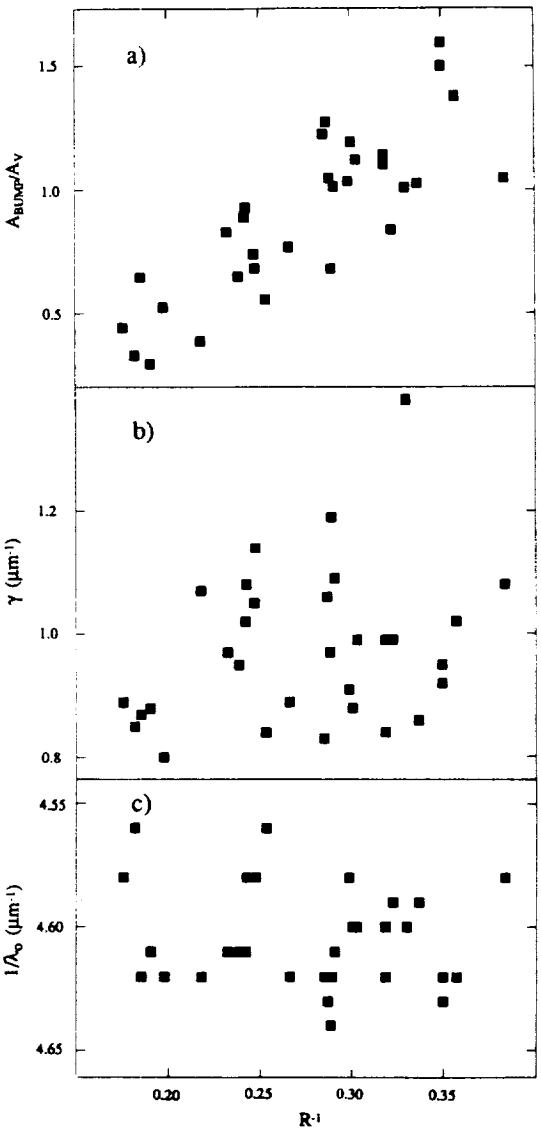

Figure 3: Three different bump parameters for the data in our sample derived by FM88. a) Absolute bump strength, A_{BUMP}, normalized to A_V, b) bump width (γ), and c) central position ($1/\lambda_o$) versus R^{-1}. The behavior shown in b) and c) implies that the bump does vary independently from the grain population responsible for variations in R.

3. COLOR EXCESS NORMALIZATION: $A_\lambda/E(\lambda_1-\lambda_2)$

The strong R-dependence in the shape of extinction curves for $\lambda < 0.7$ μm exhibited in Figure 2 implies that there exists some color excess, $E(\lambda_1 - \lambda_2)$ for $0.7\ \mu m \geq \lambda \geq 0.35$ μm, such that normalized extinction at a particular UV wavelength, $A(\lambda_{uv})/E(\lambda_1-\lambda_2)$, has a minimal dependence on R. Unfortunately, our data base requires that λ_1 and λ_2 be chosen from available broad-band or narrow-band photometry. For our sample of stars, this corresponds to the standard Johnson filters (e.g. U, B, V, or R) which may not correpond to the optimal wavelengths.

Figure 4 shows selected examples of $A(\lambda_{uv})/E(\lambda_1 - \lambda_2)$, where λ_1 and λ_2 correspond to the nominal wavelengths of the B ($\lambda \approx 0.44$ μm), V ($\lambda \approx 0.55$ μm), or R ($\lambda \approx 0.70$ μm) bandpasses, plotted against R. Figure 4a shows that A(0.18 μm)/E(B-V) exhibits a minimal R-dependence, with all but 2 points being within ≤±10% of the mean value. In Figure 4b we see that A(0.22 μm)/E(B-V) also exhibits a minimal R-dependence, with all but 4 points within ≤±10%. For E(B-V), similar results can be found for $0.24\ \mu m \geq \lambda_{uv} \geq 0.17$ μm. For λ_{uv} outside of this range, normalization by E(B-V) begins to exhibit a moderate R-dependence, as can be seen in Figure 4c for $\lambda_{uv} = 0.26$ μm. However, for this wavelength, normalization by E(B-R) produces a minimal R-dependence with all but 1 point being within ≤±10%. For E(B-R), similar results can be found for $0.30\ \mu m \geq \lambda_{uv} \geq 0.25$ μm. For $\lambda_{uv} > 0.30$ μm, normalization by E(B-R) begins to exhibit a moderate R-dependence as can be seen in Figure 4d.

One can see that normalization by some combination of color excesses utilizing B, V, and R can result in an R-independent value of $A(\lambda_{uv})/E(\lambda_1-\lambda_2)$ for $0.30\ \mu m \geq \lambda_{uv} \geq 0.17$ μm with 1-σ being <±10%. Like the analytic R-dependent results presented above, these results allow UV extinction to be estimated when direct determination is not possible or practical. However, unlike the above results, this procedure *only requires derivation of a color excess from ground-based photometry*, without the near-IR photometry which is needed to derive R.

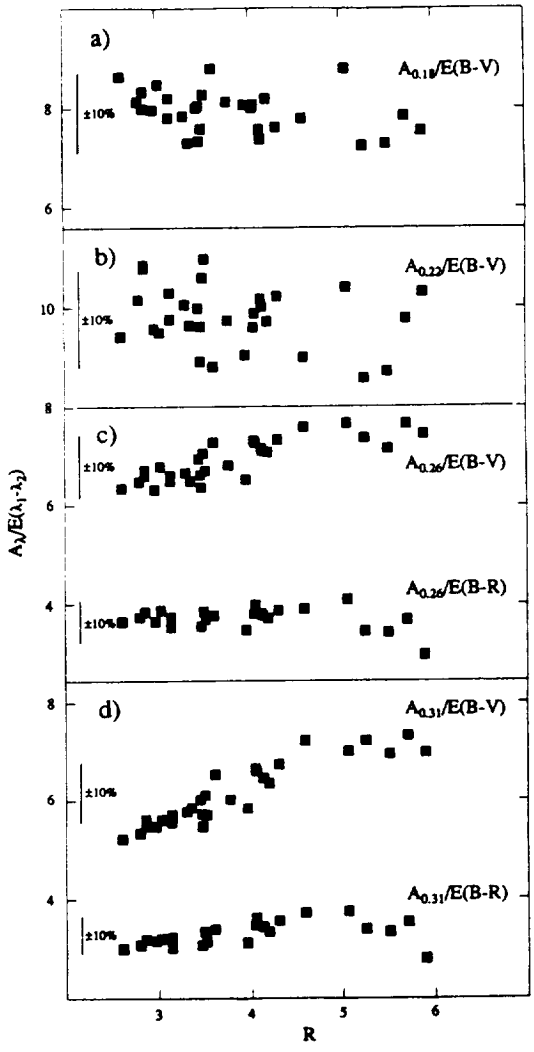

Figure 4: Values of A_λ for selected wavelengths, normalized by various color excesses. For specific wavelengths, a particular choice of color excess results in a minimal R-dependence with 1-σ <±10%. For these cases, A_λ can be estimated independent of R.

REFERENCES

Cardelli, J. A., Clayton, G. C., and Mathis, J. S.: 1988a, *Ap. J. (Lett.)*, **329**, L33 (CCM).

Cardelli, J. A., Clayton, G. C., and Mathis, J. S.: 1988b, *A Decade of UV Astronomy with the IUE Satellite*, in press.

Clayton, G. C, and Mathis, J. S.: 1988, *Ap. J.*, **327**, 911.

Fitzpatrick, E. L., and Massa, D.: 1986, *Ap. J.*, **307**, 286.

Fitzpatrick, E. L., and Massa, D.: 1988, *Ap. J.*, **328**, 734 (FM88).

Mathis, J. S., and Whiffen, G.: 1989, submitted to *Ap. J.*

Rieke, G. H., and Lebofsky, M. J.: 1985, *Ap. J.*, **288**, 618.

Schild, R. E.: 1977, *Astr. J.*, **82**, 337.

Savage, B. D., and Mathis, J. S.: 1979, *Ann. Rev. Astr. Ap.*, **17**, 73.

Seaton, M. J.: 1979, *Mon. Not. Roy. Astr. Soc.*, **187**, 73P.